Space: Science & Technology
A SCIENCE PARTNER JOURNAL

RESEARCH ARTICLE

A Legged Small Celestial Body Landing Mechanism: Landing Simulation and Experimental Test

Zhijun Zhao[1*], Shuang Wu[1], Jingdong Zhao[2*], Yaobing Wang[1], and Chuncheng Zhao[3]

[1]Beijing Key Laboratory of Intelligent Space Robotic System Technology and Applications, Beijing Institute of Spacecraft System Engineering, Beijing 100094, China. [2]State Key Laboratory of Robotics and System, Harbin Institute of Technology, Harbin 150006, China. [3]Department of Aerospace Science and Technology, Polytechnic University of Milan, Milan 20133, Italy.

*Address correspondence to: zhaojingdong@hit.edu.cn (J.Z.); zhaozhijun@aliyun.com (Z.Z.)

Citation: Zhao Z, Wu S, Zhao J, Wang Y, Zhao C. A Legged Small Celestial Body Landing Mechanism: Landing Simulation and Experimental Test. *Space Sci. Technol.* 2023;3:Article 0066. https://doi.org/10.34133/space.0066

Submitted 14 March 2023
Accepted 16 August 2023
Published 21 September 2023

Landing mechanism tends to rebound and turn over, and the stability time is long when landing on the small celestial body. Its landing performance in different conditions is necessary to be evaluated to guide the landing. Here, landing performance evaluation is realized by simulation. Key factors affecting the landing performance including cardan element damping, foot anchors, retro-rocket thrust, landing slope angle, and landing attitude are analyzed. A microgravity platform is built to test the landing mechanism, and the consistency between the simulation and the experiment is compared. On the basis of simulation and experiment, some landing suggestions are proposed to improve the landing performance.

Introduction

Landing stably is the precondition for exploring the small celestial body in situ. The surface of small body is weak gravity and irregular, and the surface environment is unknown and uncertain. The landing mechanism tends to rebound and turn over, and the landing stability time is long. This phenomenon does not exist on the moon and the Mars surface. Therefore, it is of great important to study the landing performance in different conditions to analyze the landing stability boundary, and to propose reasonable landing suggestions to support the small celestial body exploration of China.

The small celestial body landing performance research is in infancy. The Europe Space Agency simulated the landing dynamic and stability of Philae landing mechanism by Simpack software in 2000 [1]. Nanjing University of Aeronautics and Astronautics studied the landing dynamic and stability of the small celestial body landing mechanism by force analysis method in 2008 [2]. So far, most of the landing performance researches are focused on the lunar landing. The first stage was during the Apollo manned lunar landing. From 1963 to 1973, Lavender [3–6], Blanchard [7,8], Walton and colleagues [9,10], Admire and Mackey [11], Irwin [12], Hilderman et al. [13], Walton and Durling [14], Herr and Leonard [15], Zupp and Doiron [16], Otto and colleagues [17,18], and Muraca et al. [19] conducted many researches on landing performance of the lunar lander by landing dynamics analysis, simulation, and test. In addition, Nohmi and Miyahara [20] used Adams (Automatic Dynamic Analysis of Mechanical Systems) software that simulated the landing performance of SELENE-B lunar in 2005, and analyzed the influence of landing attitude, landing surface inclination, friction, and other factors on landing performance. The second stage was during the development of China's Chang'e-3 lander. Many scientific research institutions such as D. Zongquan team in Harbin Institute of Technology [21–24], N. Hong team in Nanjing University of Aeronautics and Astronautics [25–27], W. Chunjie team in Beijing University of Aeronautics and Astronautics [28,29], and Y. Jianzhong team in China Academy of Space Technology [30,31] conducted many researches on the lunar lander landing performance by landing dynamic analysis, simulation, and test. Landing performance research will progress thirdly with the development of small celestial body landing exploration.

Research methods of landing performance mainly include theoretical analysis, simulation, and test. The advantage of the theoretical analysis is that it can find out the key factors affecting the landing performance via the dynamic model, and then guide the landing mechanism design. But the correctness of the dynamic model must be verified by simulation or test. Simulation method is to establish a 3-dimensional (3D) model of the landing mechanism in Adams, Simpack, or other software to simulate the landing performance. The advantages of simulation are visual, easy to implement, and low cost. With the development of computing technology, simulation analysis has gradually become the main means of landing performance research. The test method is to study the landing dynamic and stability via the experiment. The advantage of it is high credibility, and the disadvantage is that the gravity environment of the target planet needs to be realized. Thus, the test equipment is relatively complex and the cost is high, and it is difficult to

verify all landing conditions. Generally, only typical landing conditions are tested.

Focusing on the difficulty of small celestial body landing, the paper establishes the simulation model of the landing mechanism in different landing conditions. The sensitivity of the key parameters (such as cardan element damping, landing foot slip, retro-rocket thrust, landing slope angle, and landing attitude) affecting the landing performance is analyzed. Correctness of the simulation is verified by tests. Researches on landing performance and parameter sensitivity can provide suggestions for the landing mechanism land stably on the small celestial body. The "Landing Mechanism" section introduces the structure and performance of the landing mechanism. The "Landing Simulation" section simulates the landing performance toward and away from the 30° slope. The "Key Factors Affecting the Landing Performance" section analyzes the influences of the key factors including damping, frictional coefficient, retro-rocket thrust, slope angle, and landing attitude on the landing performance. The "Landing Tests" section is the landing mechanism experimental test and its comparison with the simulation. The "Discussion" section proposes some landing suggestions based on the simulation and the tests.

Landing Mechanism

The small celestial body landing mechanism has been introduced in the paper [32]. It contains a 3-leg landing leg and an anchoring system, and its schematic is shown in Fig. 1. This design is inspired by the Rosetta lander and the ST4/Champollion lander [33,34]. The mechanical and landing parameters are shown in Table 1.

Landing mechanism contains landing foot, landing legs, cardan element, damping element, equipment base, and so on, and the landing legs are foldable. There are anchors beneath the landing foot to stop the landing mechanism from sliding when landing. The cardan element and damping element absorb the horizontal impact and vertical impact separately when landing. Furthermore, the cardan element can adjust the attitude of the equipment base after landing. A retro-rocket as a part of the control system is designed on the top of the equipment base, and it can supply a constant force lasting about 5 s toward the equipment base to prevent the landing mechanism from rebounding at the time of landing. The anchoring system can establish a connection between the small celestial body and the landing mechanism after landing to avoid it flowing away.

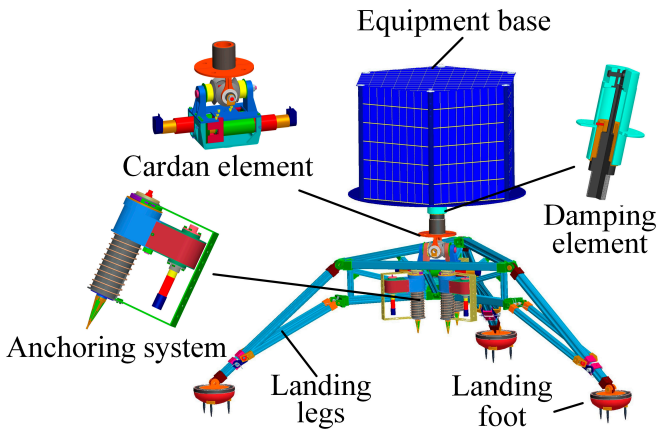

Fig. 1. Schematic of the landing mechanism.

Landing Simulation

It is difficult and complicated in ground to realize microgravity landing test. In the paper, simulation method that is used widely in the Moon and Mars lander is introduced to study the landing performance of the small celestial body landing mechanism [1]. This landing mechanism has a variety of landing velocities and attitudes, and its landing performance is evaluated when landing on 30° slope with $V_x = 0.5$ m/s, $V_z = -1.5$ m/s and $V_x = -0.5$ m/s, $V_z = -1.5$ m/s.

Landing simulation model

A 3D landing performance simulation model is designed in Adams software as shown in Fig. 2. $X_iY_iZ_iO_i$ is inertial coordinate system, and $x_ly_iz_io_l$ is body coordinate system. The rotation angle of the x_l axis around the Z_i axis is defined as yaw angle, and counterclockwise is defined as positive. Landing simulation parameters are shown in Table 2.

Landing performance is reflected by retro-rocket force, overloading acceleration and velocity of the equipment base, sliding of the landing foot, angular velocity of the landing legs, damping force and stroke of the damping element, and so on.

Some landing simulation in this section has been presented in the paper [35], and the purpose of repeat in this paper is to ensure the integrity of the paper.

Landing toward the slope

The landing mechanism will land toward the landing slope when $V_x > 0$. There are 1-2 landing mode, 2-1 landing mode, and 1-1-1 landing mode according to the contact order between the landing foot and the landing slope. The damping value of the cardan element corresponding to $V_x = 0.5$ m/s and $V_z = -1.5$ m/s is 111 Nm·s/rad. The 65 N retro-rocket force acts on the landing mechanism at the time of landing and lasts about 5 s.

1) 1-2 Landing mode: Landing simulation results of the 1-2 landing mode are shown in Fig. 3. It can be found that the

Table 1. Mechanical and landing performance parameters.

Items	Values
Mass of landing legs and landing feet	45 kg
Mass of payload	≤55 kg
Mass of anchoring system	1 kg
Horizontal velocity	-0.5 m/s ≤ V_x ≤ 0.5 m/s
Vertical velocity	$V_z \leq 1.5$ m/s
Landing slope	$\theta \leq 30°$
Tensile strength of the media	0.5 MPa ≤ τ ≤ 5 MPa
Anchoring time	≤5 s
Anchoring force	≥100 N
Penetrating velocity	20–100 m/s
Rewinding force	About 20 N
Thread length	About 2 m

landing mechanism turnover is prevented by the retro-rocket. There is no sliding of the landing feet as shown in Fig. 3D. The maximum overloading acceleration of the equipment base is 7.3*g*. Landing stability time is 3.3 s.

2) 2-1 Landing mode: Landing simulation results of the 2-1 landing mode are shown in Fig. 4. It can be found that the landing mechanism turnover is prevented by the retro-rocket. There is no sliding of the landing mechanism as shown in Fig. 4D. The maximum overloading acceleration of the equipment base is 4.3*g*. Landing stability time is 1.5 s.

3) 1-1-1 Landing mode: Landing simulation results of the 1-1-1 landing mode are shown in Fig. 5 (yaw angle is 30°). Three landing feet touch the landing slope successively. It can be found that the landing mechanism turnover is prevented by the retro-rocket. There is no sliding of the landing mechanism as shown in Fig. 5D. The maximum overloading acceleration of the equipment base is 7.5*g*. The landing stability time is 3.0 s.

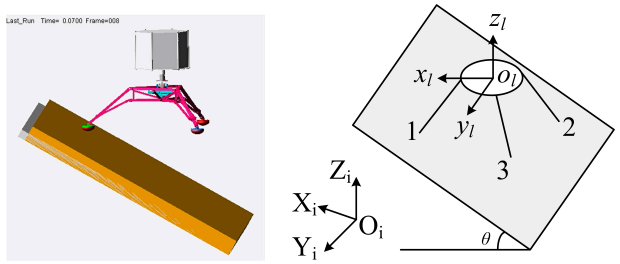

A Three-dimensional landing model **B** Coordinate system definition

Fig. 2. (A and B) Schematic of the landing simulation model.

It can be found that the 2-1 mode has a better landing performance than 1-2 and 1-1-1 modes, and 1-2 and 1-1-1 modes' landing performances are similar.

Landing away from the slope

The landing mechanism will land away from the landing slope when $V_x < 0$. The damping value of the cardan element corresponding to

Table 2. Landing simulation parameters.

Parameters	Values
Lander mass (lower cardan element)	22 kg
Lander mass (upper cardan element)	78 kg
Maximum vertical velocity V_z	–1.5 m/s
Maximum horizontal velocity V_x	–0.5 m/s and 0.5 m/s
Damping element damping c_1	900 Nm/s
Cardan element damping c_2	17–111 (Nm·s/rad)
Retro-rocket thrust T	65 N
Friction coefficient μ	2.0
Landing slope stiffness	500,000 N/m
Gravity	0*g*
Landing mode	1-2, 2-1, 1-1-1
Landing slope angle θ	30°

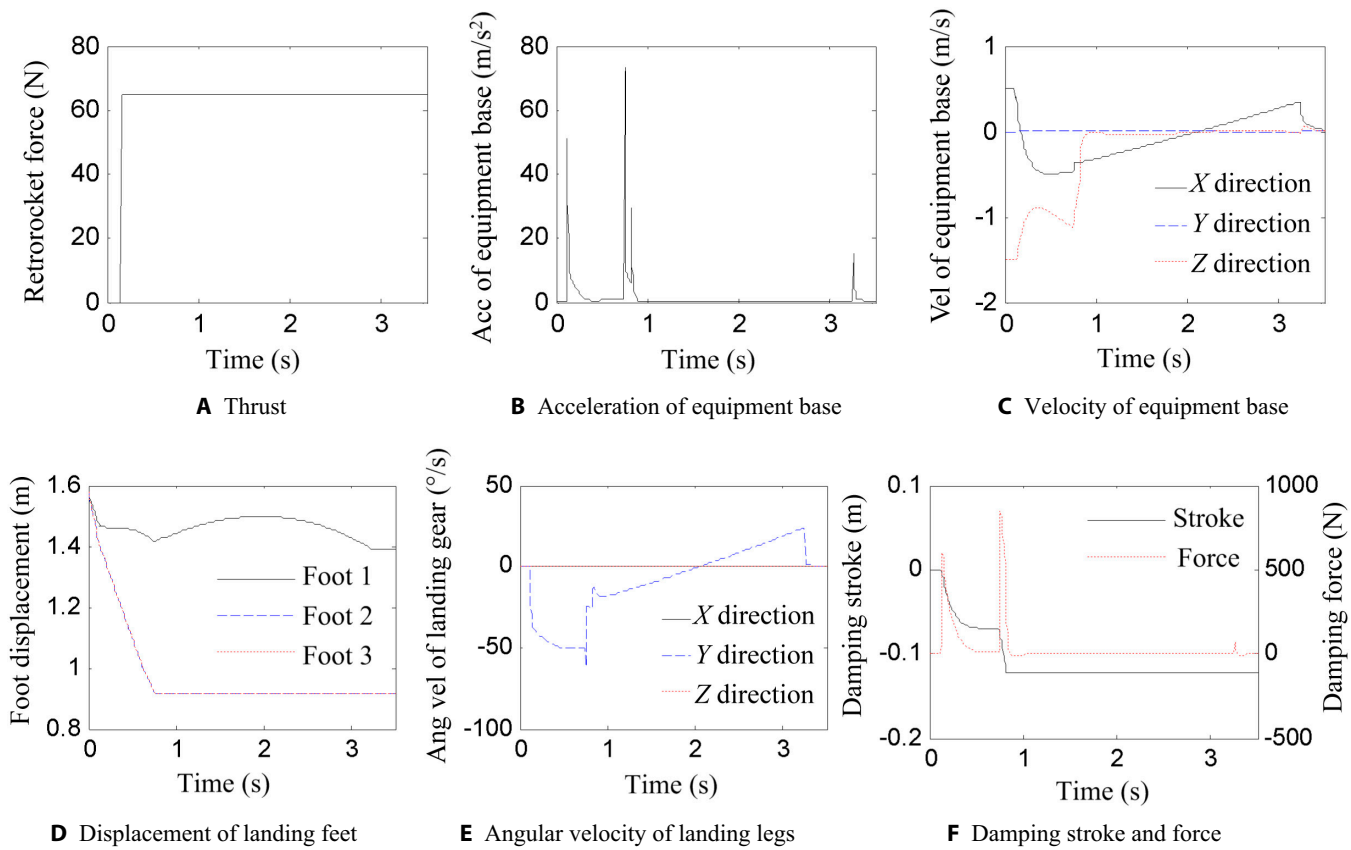

A Thrust **B** Acceleration of equipment base **C** Velocity of equipment base

D Displacement of landing feet **E** Angular velocity of landing legs **F** Damping stroke and force

Fig. 3. (A to F) Landing performance of 1-2 landing mode.

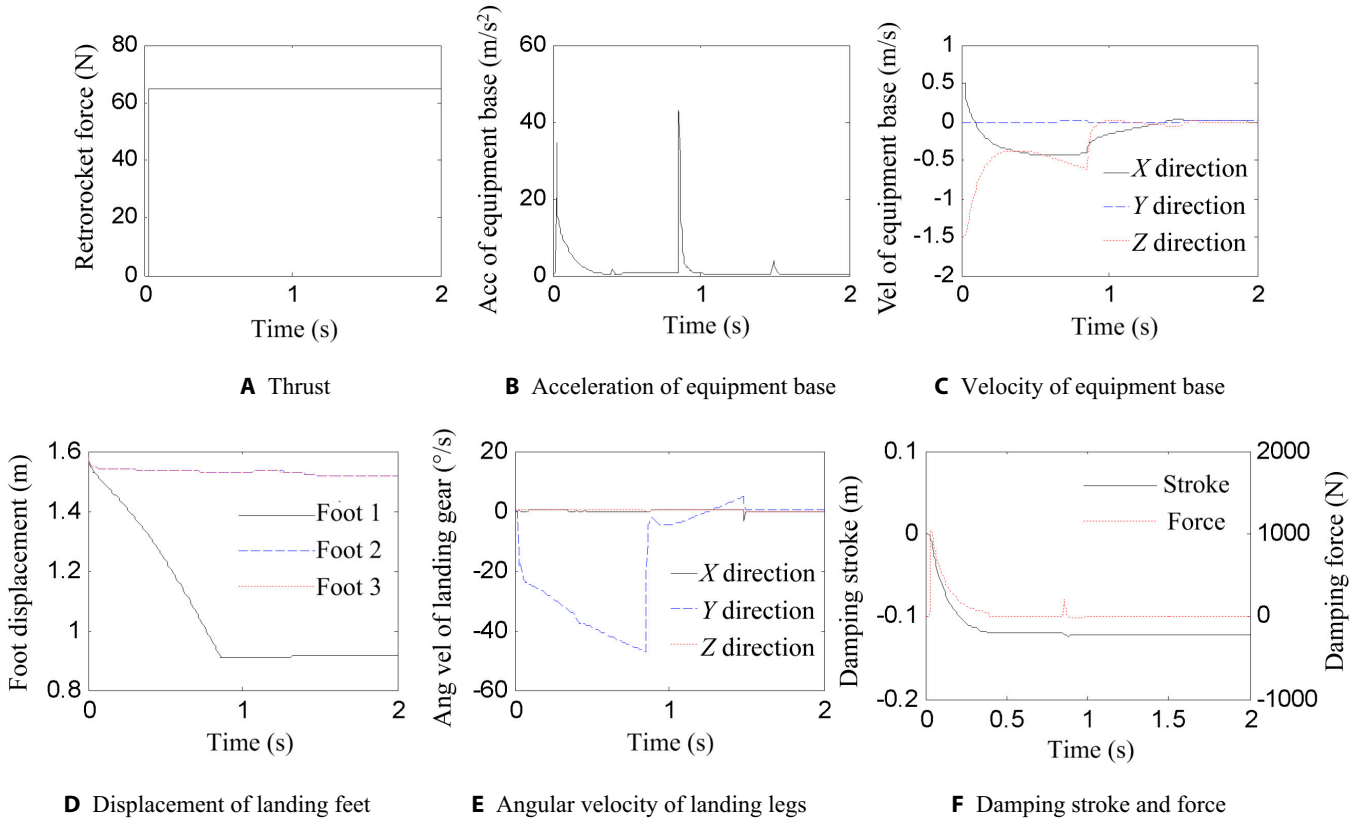

A Thrust **B** Acceleration of equipment base **C** Velocity of equipment base

D Displacement of landing feet **E** Angular velocity of landing legs **F** Damping stroke and force

Fig. 4. (A to F) Landing performance of 2-1 landing mode.

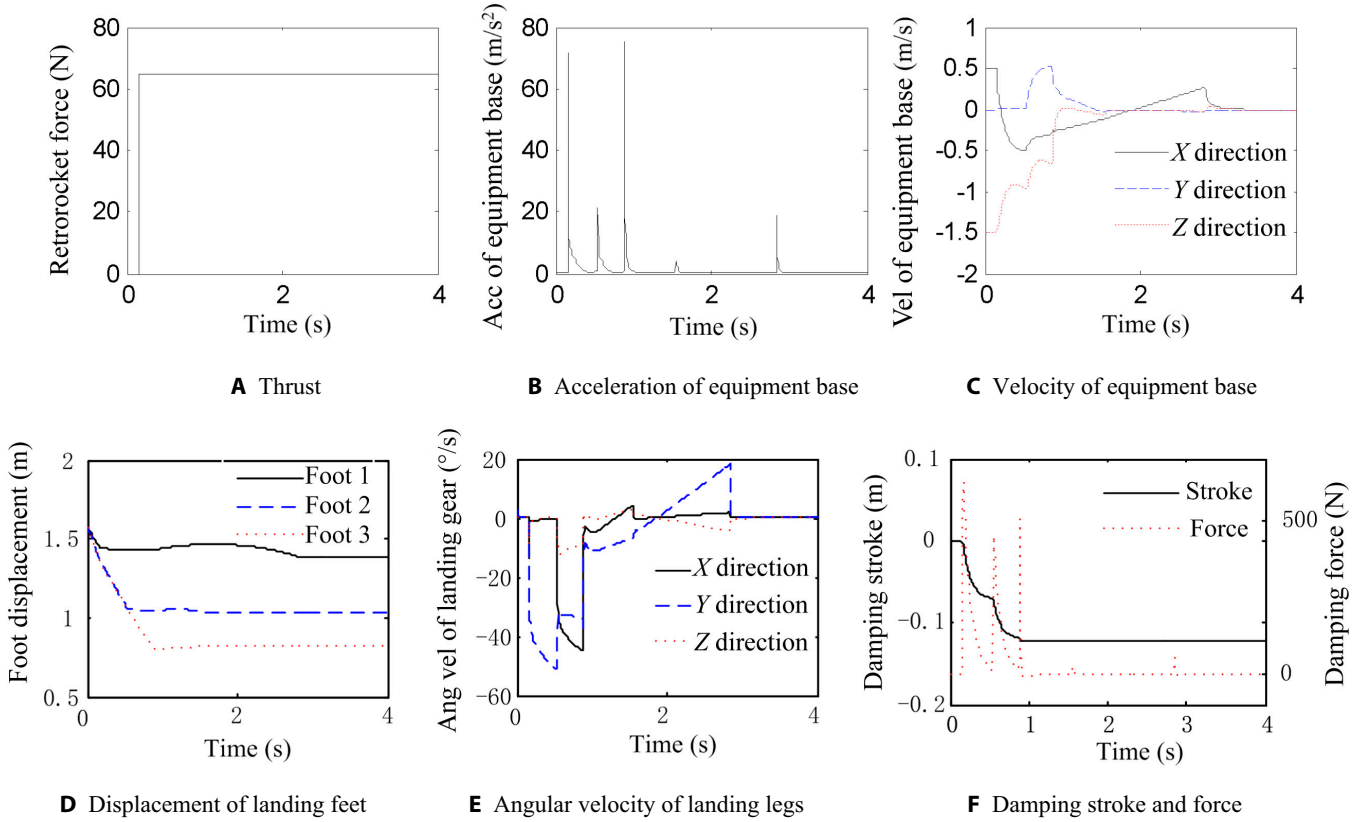

A Thrust **B** Acceleration of equipment base **C** Velocity of equipment base

D Displacement of landing feet **E** Angular velocity of landing legs **F** Damping stroke and force

Fig. 5. (A to F) Landing performance of 1-1-1 landing mode.

$V_x = -0.5$ m/s and $V_z = -1.5$ m/s is 17 Nm·s/rad. The retro-rocket force is 65 N, and it will last about 5 s.

1) 1-2 Landing mode: Landing simulation results are shown in Fig. 6. It can be found that the landing mechanism turnover is prevented by the retro-rocket. There is no sliding of the landing mechanism as shown in Fig. 6D. The maximum overloading acceleration of the equipment base is 3.7*g*. The landing stability time is 3.0 s.
2) 2-1 Landing mode: Landing simulation results are shown in Fig. 7. It can be found that the landing mechanism turnover is prevented by the retro-rocket. There is no sliding of the landing mechanism as shown in Fig. 7D. The maximum overloading acceleration of the equipment base is 2.3*g*. The landing stability time is 1.4 s.
3) 1-1-1 Landing mode: Landing simulation results are shown in Fig. 8 (yaw angle is 30°). It can be found that the landing mechanism turnover is prevented by the retro-rocket. There is no sliding of the landing mechanism as shown in Fig. 8D. The maximum overloading acceleration of the equipment base is 8.8*g*. The landing stability time is 2.5 s.

It can be found that the landing performance of the 2-1 mode is the best, the 1-2 mode is in general, and the 1-1-1 mode is the worst.

Landing performances are summarized in Table 3. The maximum overloading acceleration of the equipment base is less than 10*g*, and the landing stability time is less than 4 s. It shows that the landing mechanism can land safely in different landing conditions.

Key Factors Affecting the Landing Performance

There are many factors affecting the landing performance, such as cardan element damping, foot anchors, retro-rocket thrust, landing slope angle, landing attitude, and so on. Some of these factors are related to the structural design and some to the landing conditions. Analyzing the influence of each factor on landing performance is helpful for landing strategy proposal and landing mechanism design optimization.

Cardan element damping

There are 2 modes of the cardan element damping c_2. One is that c_2 takes a constant value, that is, the damping value is not adjusted according to the landing condition, and the other is that the value of c_2 changes according to the landing condition. When c_2 is a constant value, its control mode is simple. While c_2 is a variable value, the control mode is complex, but landing performance is better. Detailed calculation method of c_2 is introduced in [32]. In order to analyze affection of c_2, landing on 30° slope with $V_x = -0.5$ m/s and $V_z = -1.5$ m/s under 1-2, 2-1, and 1-1-1 modes is simulated. The constant value of c_2 is 111 Nm·s/rad, and the variable value of c_2 is 17 Nm·s/rad ($V_x = -0.5$ m/s, $V_z = -1.5$ m/s) [32].

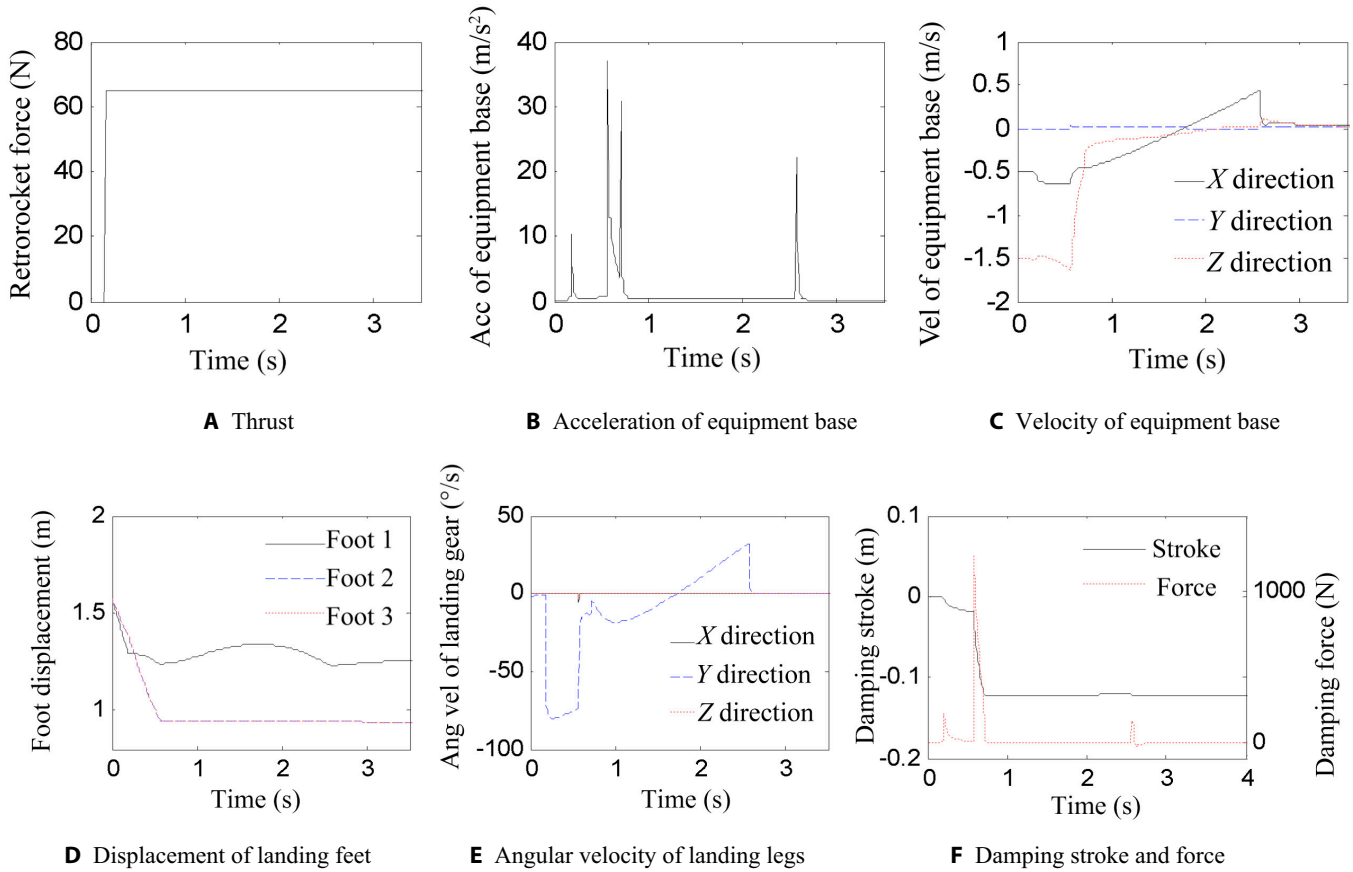

A Thrust **B** Acceleration of equipment base **C** Velocity of equipment base

D Displacement of landing feet **E** Angular velocity of landing legs **F** Damping stroke and force

Fig. 6. (A to F) Landing performance of 1-2 landing mode.

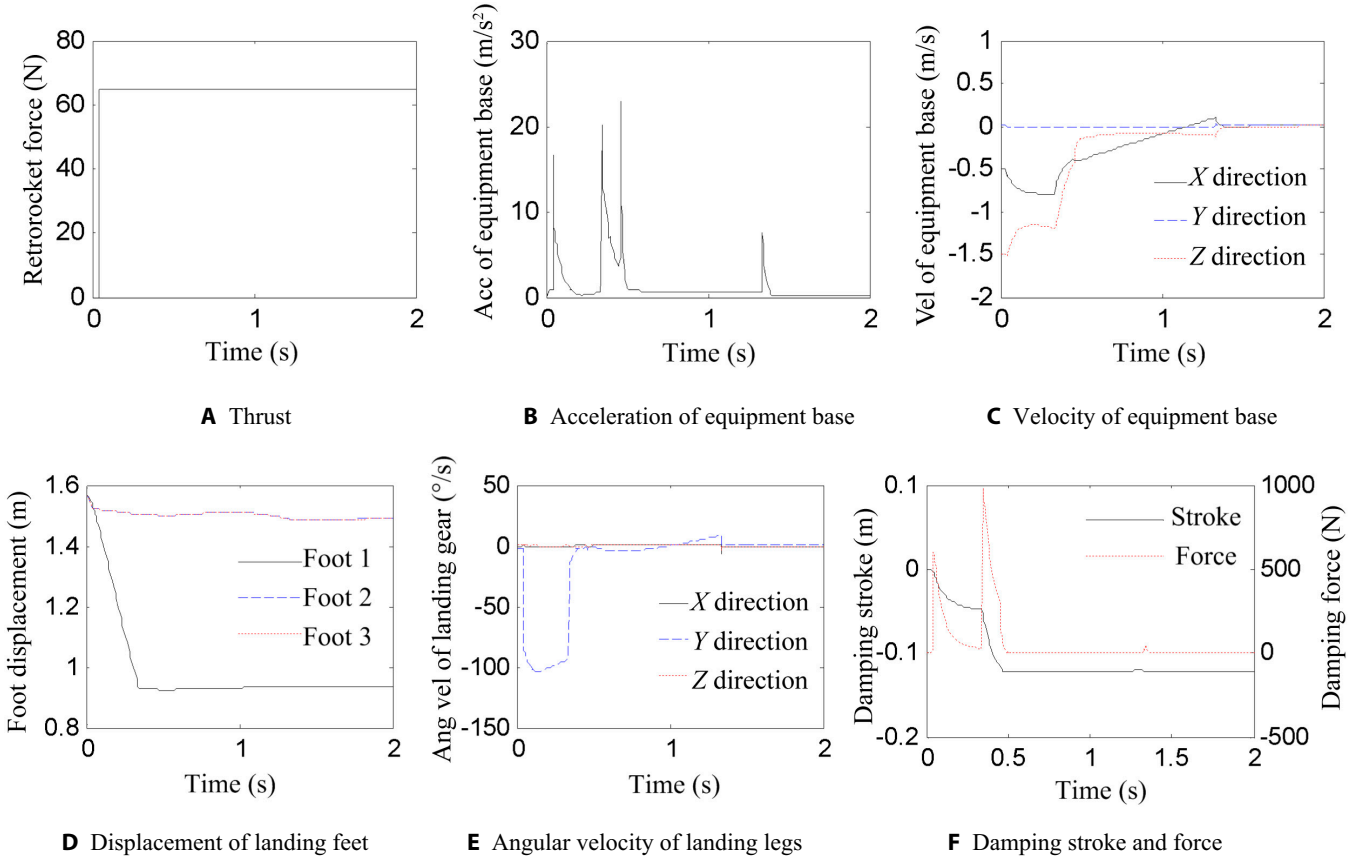

A Thrust **B** Acceleration of equipment base **C** Velocity of equipment base

D Displacement of landing feet **E** Angular velocity of landing legs **F** Damping stroke and force

Fig. 7. (A to F) Landing performance of 2-1 landing mode.

In 1-2 and 2-1 landing modes, the landing mechanism turns around the Y axis. In the 1-1-1 mode, the landing mechanism turns around X, Y, and Z axes. The acceleration of equipment base and the angular velocity of the landing legs are shown in Figs. 9 to 11. It can be seen that when c_2 is a variable value, the overloading acceleration of equipment base is weakened, and the turnover time of landing legs is shortened from 5.0 s to 2.5 s in the 1-2 mode, 2.0 s to 1.4 s in the 2-1 mode, and 4.5 s to 2.1 s in the 1-1-1 mode. Obviously, the landing stabilization time is significantly shortened and the overloading acceleration is weakened when c_2 is variable. The landing mechanism has better landing performance when c_2 is variable. Therefore, c_2 value is of great important for stable landing.

Foot anchors

The foot anchors affect the friction coefficient between landing feet and the landing surface. In order to analyze the influence of the foot anchors on the landing performance, the landing performances of the landing mechanism under 2 friction coefficients are compared. Setting the friction coefficient $\mu = 0.2$ means that there is no anchor and the friction between landing foot and the landing surface is low. Setting friction coefficient $\mu = 2.0$ means that there are foot anchors and the friction between landing feet and the landing surface is high. Landing mechanism landing on 30° slope with the maximum velocity $V_x = 0.5$ m/s and $V_z = -1.5$ m/s in the 1-2 mode is simulated, and no retro-rocket thrust is applied. The simulation results of 2 friction coefficients are shown in Fig. 12.

According to the simulation results, when $\mu = 0.2$, the landing legs turn over at the time the first landing foot touches the landing surface, and stop turning when the second and third landing feet touch the landing surface. Then, the landing mechanism slips on the landing surface. When $\mu = 2.0$, the landing mechanism begins turning when the first landing foot touches the landing surface. When the second and third landing feet touch the landing surface, the landing mechanism continues to turn and topple over. Finally, the landing mechanism leaves the landing surface and continues turning at a constant angular velocity. During the whole process, the landing mechanism does not slip on the landing surface. It can be seen that low friction is easy to induce slipping of the landing mechanism, while high friction is easy to cause the turnover of the landing mechanism. Slipping induces the landing mechanism far away from the landing point, which would affect the anchorage of the anchoring system. Friction between the landing mechanism and the landing surface should be high to avoid sliding of the landing mechanism. Overturning of landing mechanism due to high friction can be eliminated by retro-rocket thrust. Therefore, it is helpful to design foot anchors on the landing mechanism, as it can penetrate the landing surface and prevent or weaken sliding of the landing mechanism.

Retro-rocket thrust

Retro-rocket thrust is used to prevent the landing mechanism from bouncing or turning. The landing performance on 30° slope in the 1-2 mode with $V_x = 0.5$ m/s and $V_z = -1.5$ m/s is

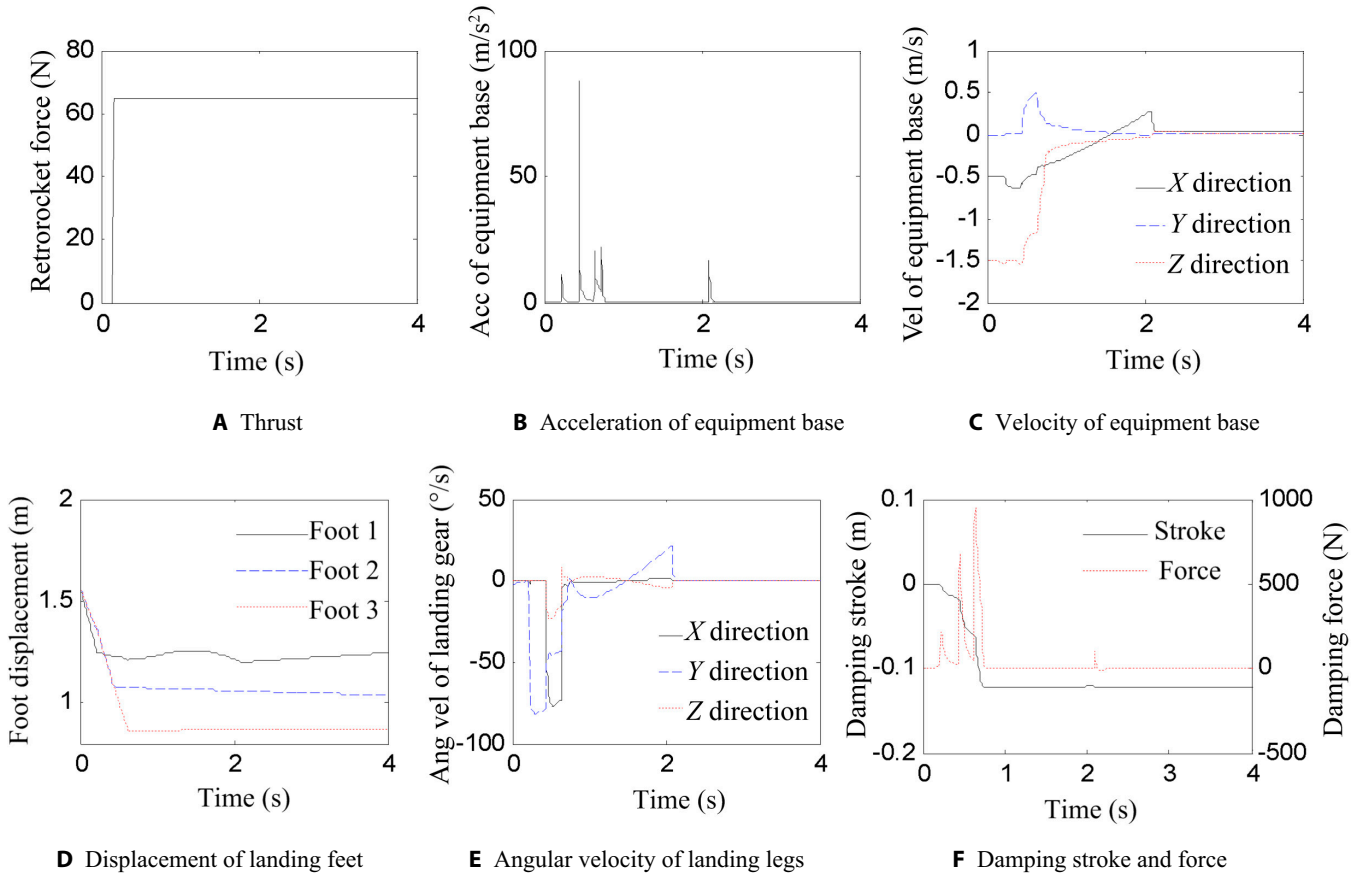

Fig. 8. (A to F) Landing performance of 1-1-1 landing mode.

Table 3. Landing simulation results summary.

Items	Landing modes	Maximum acceleration	Stability time
Toward the landing slope	1-2 mode	7.3*g*	3.3 s
	2-1 mode	4.3*g*	1.5 s
	1-1-1 mode	7.5*g*	3.0 s
Away from the landing slope	1-2 mode	3.7*g*	3.0 s
	2-1 mode	2.3*g*	1.4 s
	1-1-1 mode	8.8*g*	2.5 s

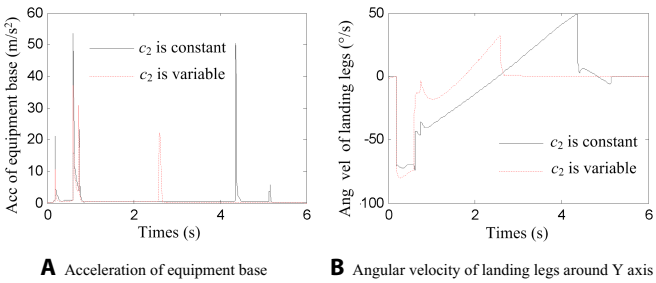

Fig. 9. (A and B) Landing performance in 1-2 mode with different cardan element damping c_2.

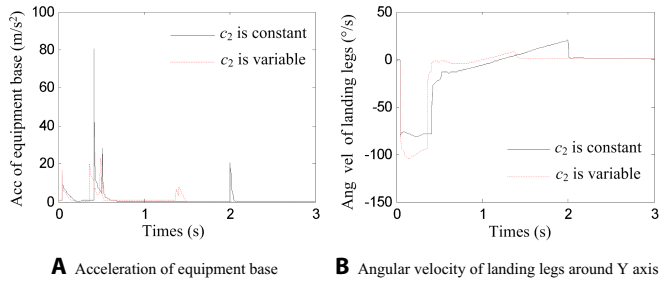

Fig. 10. (A and B) Landing performance in 2-1 mode with different cardan element damping c_2.

analyzed when $T = 0$ N and $T = 65$ N. The simulation results on different retro-rocket thrust are shown in Fig. 13. When the retro-rocket thrust $T = 0$ N, the landing mechanism turns over after the first landing foot touches the landing surface, then the second and third landing feet touch the landing surface, and the landing mechanism continues turning. Finally, the landing mechanism leaves the landing surface and continues turning at a constant angular velocity. When the retro-rocket thrust $T = 65$ N, the landing mechanism turns over after the first landing foot touches the landing surface. Due to the effect of the retro-rocket thrust, the turnover angular velocity of the landing mechanism is smaller than that of $T = 0$ N. When the second and third landing feet touch the landing surface, the landing mechanism continues turning for a period of time, and then turning angular velocity decreases to zero on the effect of

the retro-rocket thrust. Then, on the continuous action of retro-rocket thrust, 3 landing feet finally contact the landing surface. It can be seen that the turnover of the landing mechanism is eventually prevented by the retro-rocket thrust; thus, the retro-rocket thrust is helpful for landing successfully.

Landing slope

Landing performance of the landing mechanism in the 1-2 mode with $V_x = 0.5$ m/s and $V_z = -1.5$ m/s lands on 4 slopes ($\theta = 0°$, $\theta = 10°$, $\theta = 20°$, and $\theta = 30°$) is simulated. The simulation results are shown in Fig. 14. The overloading acceleration of the equipment base and the turning angular velocity of the landing legs are extracted. It can be seen that the larger the slope angle is, the higher the turning angular velocity of landing legs is, and the longer the landing stabilization time is. The influence of slope angle on equipment base overloading acceleration is not obvious. Therefore, the landing surface with smaller slope angle should be selected to reduce the landing stabilization time.

Landing attitude

The allowable maximum velocities in horizontal and vertical direction are 0.5 m/s and −1.5 m/s separately, and the maximum allowable slope angle is 30°. Landing performance on 30° slope under various landing velocities and yaw angles is analyzed. The cardan element damping is 111 Nm·s/rad, and the roll angle and pitch angle are 0°. Yaw angle increases from 0° to 120° by 10° step, and 13 landing attitudes are generated (the 13th attitude and the first attitude are theoretically the same). Each landing attitude has 10 representative landing velocities, which are (−0.5, 0, −1.5), (0.5, 0, −1.5), (0.2, 0.2, −1.5), (0.4, 0.4, −1.5), (0.5, 0.5, −1.5), (0.6, 0.6, −2), (−0.2, 0.2, −1.5), (−0.4, 0.4, −1.5), (−0.5, 0.5, −1.5), and (−0.6, 0.6, −2); the unit is m/s. Therefore, landing performances of 130 landing conditions can be obtained.

Figure 15 shows the maximum overloading acceleration of the equipment base on the above various landing conditions. It can be seen that when the landing velocity reaches (0.5, 0.5, −1.5) or (−0.5, 0.5, −1.5), the maximum overloading acceleration is close to 10*g*. The combined horizontal velocity is about 0.707 m/s, which is higher than the allowable horizontal landing velocity of 0.5 m/s. When the landing velocity is (0.6, 0.6, −2) or (−0.6, 0.6, −2), the maximum overloading acceleration is larger than 10*g*, and the horizontal landing velocity is much higher than the allowable horizontal landing velocity of 0.5 m/s. Figure 16 shows the stabilization time of the landing mechanism on the above various landing conditions. Stability time less than 10 s is considered to be landing stability. It can be seen that unstable landing will occur only when landing at (−0.6, 0.6, −2) velocity. The landing stability time on the other landing conditions is less than 5 s, and landing is stable.

In summary, when the landing mechanism lands in different landing attitudes within the allowable landing velocity, the maximum overloading acceleration is less than 10*g* and the landing stabilization time is less than 5 s. Landing performance is good. By the way, it can be seen that when the yaw angle is 60° (that is, the 2-1 landing mode), the landing mechanism has the minimum overloading acceleration and the shortest landing stability time, and the landing performance is the best.

Landing Tests

Test platform

The validity of the simulation model is verified by tests. These tests are carried out on the air-floating platform. The landing accelerations are measured by acceleration sensors. The landing attitude of the landing mechanism and the location of the sensors are shown in Fig. 17. Sensors 1, 2, and 3 are located separately on 3 landing feet, and they are used to measure impacting accelerations. Sensors 4 and 5 are located on the

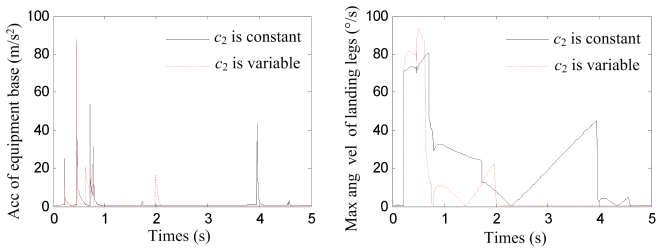

A Acceleration of equipment base **B** Maximum angular velocity of landing legs

Fig. 11. (A and B) Landing performance in 1-1-1 mode with different cardan element damping c_2.

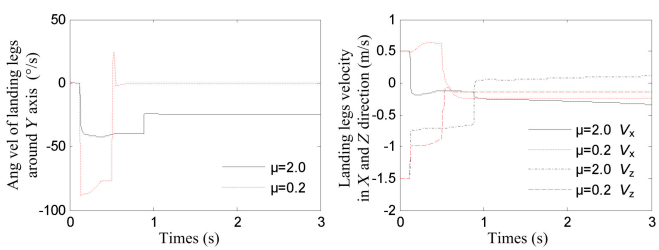

A Angular velocity of landing legs around Y axis **B** Landing legs velocity in X and Z direction

Fig. 12. (A and B) Landing performances of different friction coefficients.

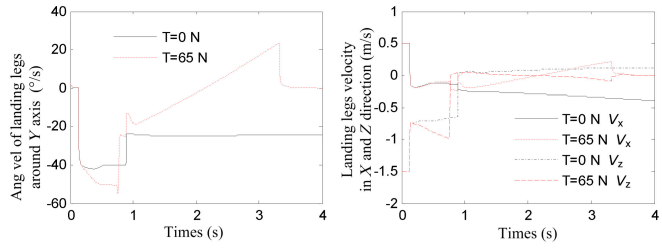

A Angular velocity of landing legs around Y axis **B** Landing legs velocity in X and Z direction

Fig. 13. (A and B) Landing performances with and without retro-rocket thrust.

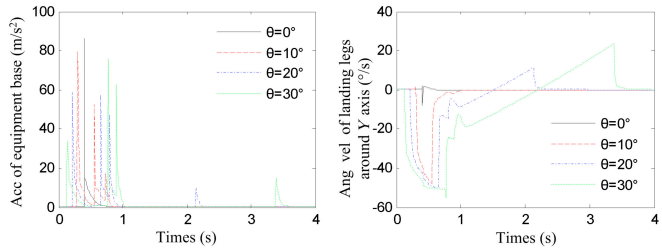

A Acceleration of equipment base **B** Angular velocity of landing leg around Y axis

Fig. 14. (A and B) Landing performances on different slopes.

equipment base and are used to measure their acceleration in landing and horizontal direction. A gyroscope is used to measure the attitude of the of the equipment base.

Test and simulation comparison

Landing performances on 30° slope with $V_y = 1.54$ m/s (high-speed landing) in 1-2, 2-1, and 1-1-1 modes are tested separately. These landing modes and velocities are imported into the simulation model. Landing performances between test and simulation are compared.

(1) Landing on 30° slope in the 1-2 mode

When landing on a 30° slope with −1.54 m/s vertical velocity in the 1-2 mode, test and simulation results of the landing mechanism are shown in Fig. 18. Figure 18A shows the overloading acceleration of the equipment base. It can be seen that the overloading acceleration of the equipment base obtained by simulation is close to that obtained by test, and the simulation result is slightly larger than the test. This is due to the mechanical flexibility of the landing mechanism, which will produce flexible deformation in the test and absorb part of the impact load. Figure 18B shows the landing leg turnover angular velocity and turnover angle. It can be seen that the changes of landing leg turnover angular velocity and turnover angle in simulation and test are relatively consistent. But at the time between about 0.7 and 2.5 s, landing leg turnover angle in test is less than that in simulation. The reason is that landing surface in test is hard wood and the foot anchors fail to penetrate the hard wood, which results in slight slip of the landing mechanism. Thus, landing leg turnover angle is smaller than that in simulation.

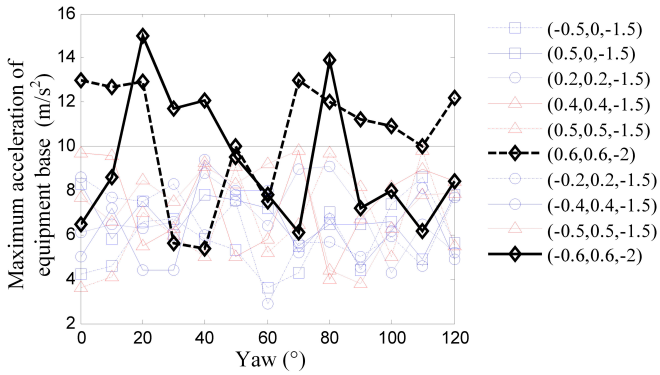

Fig. 15. Maximum overloading acceleration of equipment base in different yaw angles and landing velocities.

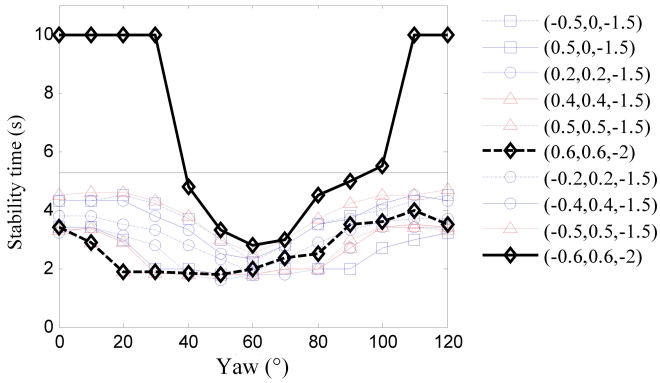

Fig. 16. Stability time of the landing mechanism in different yaw angles and landing velocities equipment base.

(2) Landing on 30° slope in the 2-1 mode

When landing on 30° slope with −1.54 m/s vertical velocity in the 2-1 mode, test and simulation results of the landing mechanism are shown in Fig. 19. Figure 19A shows the overloading acceleration of the equipment base. It can be seen that the overloading acceleration of the equipment base obtained by simulation is close to that obtained by test, and the simulation result is slightly larger than the test. The reason for this phenomenon is the same as that for landing in the 1-2 mode. Figure 19B shows the landing leg turnover angular velocity and turnover angle obtained by simulation and test. It can be seen that the changes of landing leg turnover angular velocity and turnover angle in simulation and test are relatively consistent. But at the time between about 0.5 and 2 s, landing leg turnover angle in test is less than that in simulation for the same reason as that in the 1-2 mode. In addition, when the landing feet hit the landing surface for the first time, the landing leg turnover angular velocity in simulation is larger than that in test. This is related to the fact that there is friction between the landing feet and the landing legs, and this friction is ignored in simulation but existed in test.

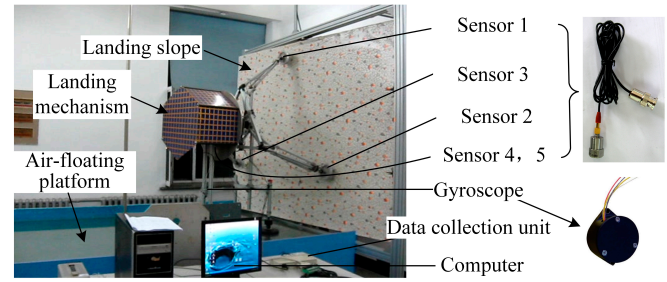

Fig. 17. Landing mechanism on the air-floating platform.

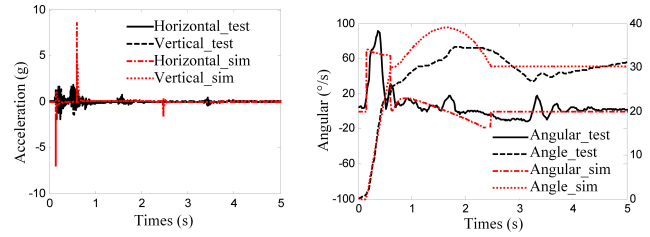

A Overloading acc of equipment base **B** Turning angular velocity and angle of landing legs

Fig. 18. (A and B) Results of test and simulation when $\theta = 30°$ and $V_y = -1.54$ m/s in 1-2 mode.

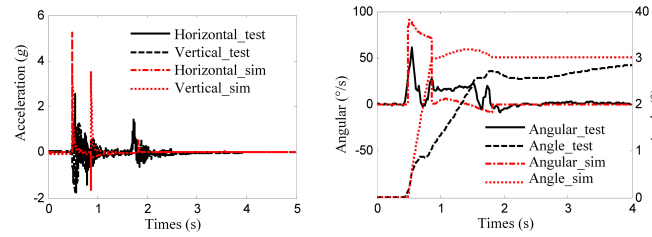

A Overloading acc of equipment base **B** Turning angular velocity and angle of landing legs

Fig. 19. (A and B) Results of tests and simulation when $\theta = 30°$ and $V_y = -1.54$ m/s in 2-1 mode.

(3) Landing on 30° slope in the 1-1-1 mode

When landing on a 30° slope with −1.54 m/s vertical velocity in the 1-1-1 mode, test and simulation results of the landing mechanism are shown in Fig. 20. Figure 20A shows the overloading acceleration of the equipment base. It can be seen that the overloading acceleration of the equipment base obtained by simulation and test is close to each other, and the simulation result is slightly larger than the test. The reason for this phenomenon is the same as that for landing in the 1-1-1 mode. Figure 20B shows the landing leg turning angular velocity and turnover angle obtained by simulation and test. It can be seen that the changes of landing leg turning angular velocity and turnover angle in simulation and test are relatively consistent. However, landing leg turnover angle and turnover angular velocity in test are both smaller than those in simulation. The reasons are the same as those in 1-2 and 2-1 landing modes. In addition, the overturning angle of the landing legs around 3 s becomes smaller in test than in simulation. This is due to the slight rebound of the landing legs when the third landing foot touched the landing surface, which results in a smaller turning angle of the landing legs relative to the landing surface.

Overloading acceleration of the equipment base and the stability time of the landing mechanism obtained by tests are shown in Table 4. It can found that the 2-1 landing mode has the shortest stability time, and there is no obvious relationship between the overloading acceleration and the landing mode. This conclusion is the same as that in simulation.

Discussion

Landing performance simulations and tests are carried out on the small celestial body landing mechanism, and the key factors affecting the landing performance are analyzed. The landing stability time of the 3-legged landing mechanism proposed in this paper is less than 6 s, and the overloading acceleration is less than 10*g*. Landing performances evaluated by simulations and tests are consistent and reasonable. The following methods are helpful to improve landing performance: (a) Three legs landing mechanism should preferentially choose the 2-1 landing mode. (b) Adjustable damping corresponding to landing conditions is helpful to improve the landing stability. (c) Foot anchors can reduce landing slip and shorten landing stabilization time. (d) Retro-rocket on top of the landing mechanism can weaken or prevent rebounding when landing. (e) The landing mechanism should preferentially land on flat areas.

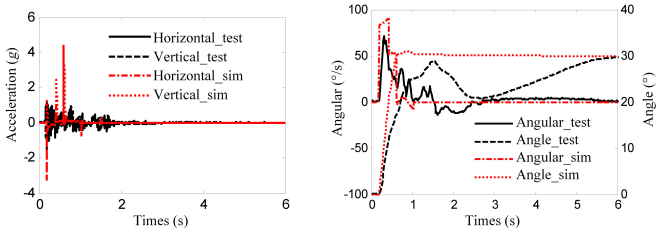

A Overloading acc of equipment base **B** Turning angular velocity and angle of landing legs

Fig. 20. (A and B) Results of tests and simulation when $\theta = 30°$ and $V_y = -1.54$ m/s in 1-1-1 mode.

Table 4. Overloading accelerations of the equipment base and stability time of the landing mechanism.

Landing mode	Vertical overloading acceleration	Horizontal overloading acceleration	Stability time
θ = 30°, 1-2 mode	1.8*g*	2.0*g*	5.5 s
θ = 30°, 2-1 mode	2.6*g*	1.8*g*	3.5 s
θ = 30°, 1-1-1 mode	1.3*g*	1.5*g*	5.5 s

Acknowledgments

Funding: This work is financially supported by the National Natural Science Foundation of China (no. U22B2080) and the State Key Laboratory of Robotics and System (HIT) (no. SKLRS-2021-KF-14). **Competing interests:** The authors declare that there is no conflict of interest regarding the publication of this article.

Data Availability

The data are available from the authors upon a reasonable request.

References

1. Hilchenbach M, Kuchemann O, Rosenbauer H. Impact on a comet: Rosetta Lander simulations. *Planet Space Sci*. 2000;48(5):361–369.
2. Wu ZB. Design and research on the anchoring mechanism of small body landing mechanism. *Nanjing Univ Aeronaut Astronaut*. 2008;33–66.
3. Lavender RE. Equations for two-dimensional analysis of touchdown dynamics of spacecraft with hinged legs including elastic, damping and crushing effects. NASA-TM-X-57404. 1963 Nov 6;1–33.
4. Lavender RE. Touchdown dynamics analysis of spacecraft for soft lunar landing. NASA TN. 1964;D-2001:1–41.
5. Lavender RE. On touchdown dynamics analysis for lunar landing. Proceedings of AIAA Symposium on Structural Dynamics and Aeroelasticity. 1965. https//:ntrs.nasa.gov/citations/19650052928.
6. Lavender RE. Monte Carlo approach to touchdown dynamics for soft lunar landings. NASA TN. 1965. https//:ntrs.nasa.gov/citations/19660001460.
7. Blanchard UJ. Characteristics of a lunar landing configuration having various multiple-leg landing-gear arrangements. NASA-TN-D-2027. 1964. https://ntrs.nasa.gov/citations/20070030982.
8. Blanchard UJ. Full-scale dynamic landing-impact investigation of a prototype lunar module landing gear. NASA-TN-D-5029. 1969. https://ntrs.nasa.gov/citations/19690011603.
9. Walton WC, Herr RW, Leonard HW. Studies of touchdown stability for lunar landing vehicles. *J Spacec*. 1964;1(5):552–556.
10. Walton WC, Durling BJ, Leonard HW. Application of digital computer techniques to the study of the impact dynamics of lunar-landing vehicles. 1964; N66-15238:https://ntrs.nasa.gov/citations/19660005949.

11. Admire J, Mackey A. *Dynamic analysis of a multi-legged lunar landing vehicle to determine structural loads during touchdown*. Washington (DC): National Aeronautics and Space Administration; 1965. p. 1–36.
12. Irwin DC. Landing dynamics study for lunar landing research vehicle. NASA CR-428. 1965. https://ntrs.nasa.gov/api/citations/19660014158/downloads/19660014158.pdf.
13. Hilderman RA, Mueller WH, Mantus M. Landing dynamics of the lunar excursion module. *J Spacec*. 1966;3(10):1484–1489.
14. Walton CW, Durling BJ. A procedure for computing the motion of a lunar-landing vehicle during the landing impact. NASA TN. 1967. https://ntrs.nasa.gov/citations/19670029079.
15. Herr RW, Leonard HW. Dynamic model investigation of touchdown stability of lunar-landing vehicles. NASA-TND-4215. 1967. https://ntrs.nasa.gov/citations/19670029284.
16. Zupp GA, Doiron HH. A mathematical procedure for predicting the touchdown dynamics of a soft-landing vehicle. NASA TND-7045. 1971. https://ntrs.nasa.gov/api/citations/19710007293/downloads/19710007293.pdf.
17. Otto O R, Laurenson R M, Melliere R A, et al. Analyses and limited evaluation of payload and legged landing system structures for the survivable soft landing of instrument payloads. NASA CR-111919. 1971. p. 1–496.
18. Laurenson RM, Melliere RA, Mcgehee JR. Analysis of legged landers for the survivable soft landing of instrument payloads. *J Spacecraft*. 1973;10(3):208–214.
19. Muraca RJ, Campbell JW, King CA. A Monte Carlo analysis of the Viking Lander dynamics at touchdown. *NASA TN*. 1975;D-7959:1–57.
20. Nohmi M, Miyahara A. Modeling for lunar lander by mechanical dynamics software. Paper presented at: AIAA Modeling and Simulation Technologies Conference and Exhibit; 2005; San Francisco, CA. p. 1–9.
21. Wang SC, Deng ZQ, Hu M, Gao HB. Dynamic model building and simulation for mechanical Main body of lunar Lander. *J Cent South Univ*. 2005;12(3):329–334.
22. Deng ZQ, Wang SC. Experimental research on buffer characteristics of lunar Lander with three legs. *J Harbin Inst Technol*. 2007;39(1):32–34.
23. Wang C, Liu RQ, Qeng ZQ. Dynamic analysis of lunar lander's landing process. *J Bejing Univ Aeronaut Astronaut*. 2008;34(4):381–385.
24. Luo CJ, Deng ZQ, Liu RQ. Landing stability investigation of legged-type spacecraft Lander based on zero moment point theory. *J Mech Eng*. 2010;46(9):38–45.
25. Chen JB, Wan JL, Li LC, Nie H. Analysis on the influencing factors of performance in lunar Lander. *J Astronaut*. 2010;31(3):669–673.
26. Chen JB, Nie H, Wan JL. Digital design and landing performance influence factors of deep space Lander. *Chin J Aeronaut*. 2014;35(2):541–554.
27. Chen JB, Nie H. Overloading of landing based on the deformation of the lunar Lander. *Chin J Aeronaut*. 2008;21:43–47.
28. Lu YT, Song SG, Wang CJ. Dynamic analysis for lunar lander based on rigid-flexible coupled model. *J Bejing Univ Aeronaut Astronaut*. 2010;36(11):1348–1352.
29. Wang JJ, Wang CJ, Song SG. Performance optimization of lunar lander based on response surface methodology. *J Bejing Univ Aeronaut Astronaut*. 2014;40(5):707–711.
30. Zhu W, Yang JZ. Touchdown stability simulation of landing gear system for lunar Lander. *J Astronaut*. 2009;30(5):1792–1796.
31. Jiang WS, Huang W, Shen ZW, et al. Soft landing dynamics simulation for lunar explorer. *J Astronaut*. 2011;32(3):462–469.
32. Zhao ZJ, Zhao JD, Liu H. Landing dynamic and key parameter estimations of a landing mechanism to asteroid with soft surface. *Interl J Aeronaut Space Sci*. 2013;14(3):237–246.
33. Max-Planck-Institut fur aeronomie 2000-2001. MPAE Report. 2001. p.140–153.
34. Steltzner AD, Nasif AK. Anchoring technology for in situ exploration of small bodies. Paper presented at: 2000 IEEE Aerospace Conference; 2020 Mar 25; Big Sky, MT.
35. Zhao Z J, Li D L, Yuan B F. Landing performance simulation of an asteroid landing mechanism. Paper presented at: Proceeding of the 2015 IEEE International Conference on Information and Automation; 2015; Lijiang, China. p. 1914–1919.